Outskirts of Galaxy Clusters: Intense Life in the Suburbs
Proceedings IAU Colloquium No. 195, 2004
A. Diaferio, ed.

DOI: 10.1017/S174392130400119X

Effects of small-scale structure on the progress and duration of reionization

Ilian T. Iliev[1], Paul R. Shapiro[2], Evan Scannapieco[3] and Alejandro C. Raga[4]

[1]Canadian Institute for Theoretical Astrophysics, University of Toronto, 60 St. George Street, Toronto, ON M5S 3H8, Canada e-mail: iliev@cita.utoronto.ca

[2]Department of Astronomy, University of Texas, Austin, TX 78712-1083

[3]Kavli Institute for Theoretical Physics, Kohn Hall, UC Santa Barbara, Santa Barbara, CA 93106

[4]Instituto de Ciencias Nucleares, Universidad Nacional Autonoma de México (UNAM), Apdo. Postal 70-543, 04510 México, D. F., México

Abstract. The propagation of cosmological ionization fronts during the reionization of the universe is strongly influenced by small-scale ($\sim$ kpc) gas inhomogeneities caused by structure formation. In this paper we study this important effect by performing detailed radiative-hydrodynamic simulations of photoevaporation of cosmological minihalos (MHs) and incorporating the results into a semi-analytical model of reionization, which also includes the effect of mean intergalactic medium (IGM) clumping and the nonlinear clustering of minihalos. We find that small-scale structures have a significant effect on the process of reionization, slowing it down and extending it in time. This can help in understanding the recent observations by the Wilkinson Microwave Anisotropy Probe (WMAP) satellite, which point to an early and extended reionization epoch.

The hierarchical Cold Dark Matter model predicts that small-scale structures form in abundance at redshifts below $z \sim 20$, during the Dark Ages and the subsequent epoch of reionization [Fig. 1 (a)]. The rare highest peaks in the density field collapse into virialized halos with temperatures $T_{\rm vir} \gtrsim 10^4$ K. Since the gas in such halos is able to cool efficiently through atomic cooling and form stars or host QSOs, they represent the most likely ionization sources for reionization. Meanwhile the much more abundant lower-mass peaks collapse to form minihalos, which are unable to cool efficiently and thus remain largely inert and neutral. Finally, the remainder of the IGM is also strongly clumped in filaments, not-yet-collapsed halos and other structures.

The first ionizing sources start to appear around $z \sim 20-30$, forming H II regions around themselves, and expanding R-type ionization fronts (I-fronts) into the surrounding neutral IGM. These I-fronts propagate until finally the ionized regions percolate and overlap, thus completing reionization around $z \sim 6$. When an I-front encounters a minihalo, it slows down to a slow, D-type I-front and gets trapped. Thereafter it only slowly works its way in through the minihalo, heating and ionizing its gas and blowing a supersonic wind into the IGM back towards the source. Correct modeling of this complicated process requires high-resolution hydrodynamic and radiative transfer simulations, which we have performed with a 2-D adaptive-grid code, CORAL (Shapiro et al. 2004; Shapiro and Raga 2004) which we developed. The main results obtained include the dependences of the evaporation time $t_{\rm ev}$ and ionizing photon consumption per minihalo atom ξ on minihalo parameters and source fluxes and spectra [Fig. 1 (b)], which we used to construct a semi-analytical model to study the effect of minihalo photoevaporation on the progress and duration of reionization (Iliev et al. 2004) as follows. The evolution

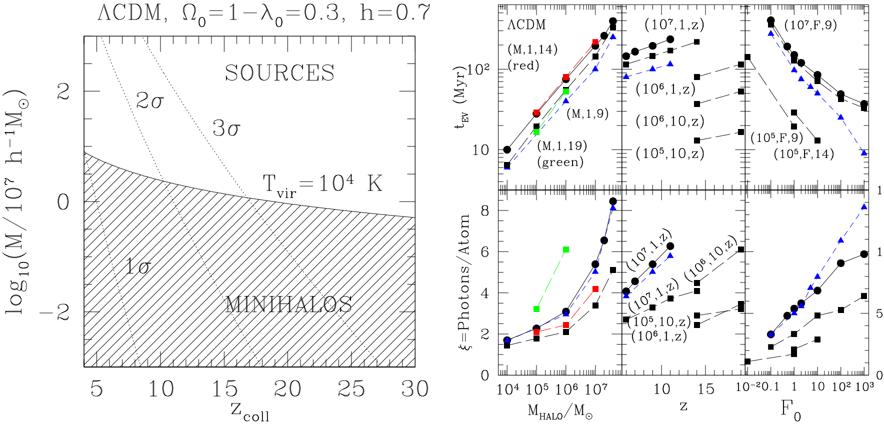

Figure 1. (a)(left) How common are minihalos and ionizing sources at high redshift? Shaded region represents minihalos, while dotted curves represent $\nu - \sigma$ fluctuations with $\nu = 1$ (most common), 2 and 3, from the Press-Schechter formalism (Press and Schechter 1974). (b) (right) Individual minihalos' photoevaporation times $t_{\rm ev}$ (top panels) and total ionizing photon consumption per minihalo atom ξ (bottom panels) vs. halo mass M (left), redshift of collapse of the halo z (middle) and dimensionless ionizing flux (right), with $F_0 \equiv F/(10^{56}{\rm s}^{-1}/[4\pi(1\,{\rm Mpc})^2])$. Symbols represent 5×10^4 K black-body (circles), QSO (triangles) and 10^5 K black-body (squares) spectra labeled by (M, F_0, z) with the parameters kept fixed in each case indicated.

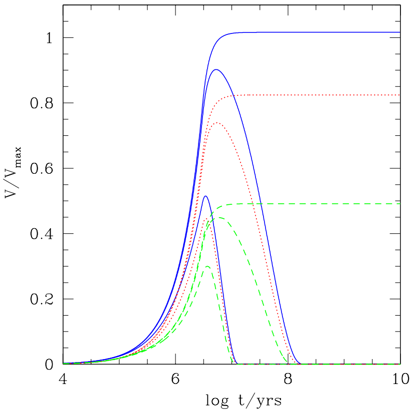

Figure 2. The evolution of the volume of the H II region about a single source of mass $10^8 M_\odot$ forming at $z = 15$. Cases of no MHs (solid), unbiased MHs (dotted), and biased MHs (dashed) for IGM clumping factors (top to bottom in each case) $C = 0$ (i.e. no recombinations in IGM gas), 1 (mean IGM), and 10 (clumped IGM). $V_{\rm max}$ is the maximum ionized volume reached during the lifetime of the source (~ 3 Myr) in the $C = 0$, no MHs case.

of the ionized volume around a source of a given luminosity through a clumpy IGM with a constant volume-averaged clumping factor, $C \equiv \langle n^2\rangle/\langle n\rangle^2$ was first derived in Shapiro & Giroux (1987). Strong gas clumping significantly increases the recombination rate, thus decreasing the ionizing flux that reaches the I-front through the clumpy H II region. We followed a similar approach, modifying it appropriately to account for the increased ionizing photon consumption from minihalos using the small-scale simulation results presented above. Furthermore, we included the effect of source screening by the

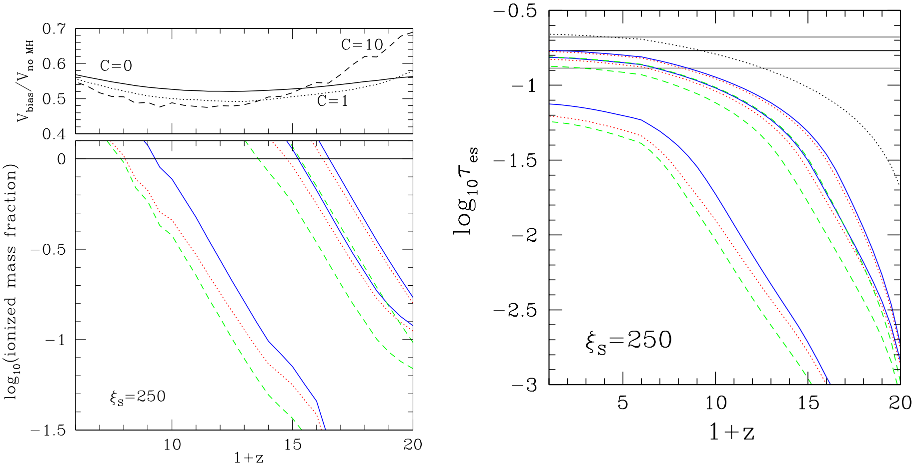

Figure 3. (a) (left) (bottom panel) Logarithm of ionized mass fractions (0='overlap'). Same notation as in Fig. 2. (upper panel) Ratios of the ionized volume fractions in the presence of biased minihalos and with no minihalos for $C = 0$, 1 and 10. Sources with lifetime $t_s = 3$ Myr producing a total of 250 photons/atom are assumed in both (a) and (b). (b) (right) Optical depth due to electron scattering $\tau_{\rm es}$ integrated from $z = 20$ down vs. redshift z. Same cases and notation as in (a). Top curve shows the optical depth produced assuming complete ionization from $z = 20$ on. Horizontal lines indicate the best-fit and $1 - \sigma$ uncertainties of the first-year WMAP result $\tau_{\rm es} = 0.17 \pm 0.04$.

biased distribution of the surrounding minihalos, using the method of Scannapieco & Barkana (2002). This biasing effect is particularly important at high redshifts where the source halos lie in rare high peaks of the density field, around which minihalos cluster strongly, thereby increasing their ionizing photon consumption due to the increased flux as compared to the unbiased case. In Fig. 2 we show an illustrative example. Presence of biased minihalos decreases the ionized volume by a significant factor of ~ 2, more than twice the decrease in the unbiased case. We have then used these individual-source results to model the global reionization process, as follows. We find the number density of sources and their mass distribution based on the PS formalism and calculate and add-up the ionized volumes around each source according to the method described above. Complete reionization is reached when the ionized regions volume-filling factor becomes one. Sample results are shown in Fig. 3, indicating that minihalos can delay reionization by $\Delta z \sim 1 - 2$, while high IGM gas clumping can have an even stronger effect, further delaying reionization. This particular model is consistent at $1 - \sigma$ level with the current WMAP results for the electron-scattering optical depth $\tau_{\rm es}$ for unclumped IGM gas, but has too low electron-scattering optical depth for clumped IGM [Fig. 3 (b)]. A further detailed study of the parameter space is required to quantify better the WMAP constraint on the process of reionization in presence of small-scale structures.

References

Iliev, I. T., Scannapieco, E. & Shapiro, P. R. 2004, in preparation
Iliev, I. T., Shapiro, P. R. & Raga, A. C. 2004, in preparation
Press, W. H., & Schechter, P. 1974, ApJ, **187**, 425 (PS)
Scannapieco, E. & Barkana, R. 2002, ApJ,**571**, 585
Shapiro, P. R. & Giroux, M. L., 1987, ApJ, **321**, L107
Shapiro P. R., Iliev I. T. & Raga A. C. 2004, MNRAS, **348**, 753

Fernando Atrio-Barandela and Rashid Sunyaev *(by G. Murante).*

John Stocke and Gustavo Yepes *(by G. Murante).*

Marc Voit and Sergei Shandarin. In the background, Ravi Sheth and Antonaldo Diaferio gossip *(by A. Ferrari).*